



ISSN: 2348-5906
CODEN: IJMRK2
IJMR 2014; 1 (4): 17-24
© 2014 IJMR
Received: 17-07-2014
Accepted: 30-08-2014

Bhagath Kumar Palaka
Centre for Bioinformatics
Pondicherry University
Puducherry-605014, India
Email:
bhagath.palaka@gmail.com

Nagendra Pratap Singh
Centre for Bioinformatics
Pondicherry University
Puducherry-605014, India

Kasi Viswanath Kotapati
Centre for Bioinformatics
Pondicherry University
Puducherry-605014, India

Sampath Kumar Ranganathan
Centre for Bioinformatics
Pondicherry University
Puducherry-605014, India

Dinakara Rao Ampasala
Associate Professor
Centre for Bioinformatics
Pondicherry University
Puducherry-605014, India
Email: ampasaladr@bicpu.edu.in

For Correspondence:
Dinakara Rao Ampasala
Associate Professor
Centre for Bioinformatics
Pondicherry University
Puducherry-605014, India
Email:
ampasaladr@bicpu.edu.in

UDP-N-Acetyl glucosamine pyrophosphorylase as novel target for controlling *Aedes aegypti* – molecular modeling, docking and simulation studies

Bhagath Kumar P., Nagendra Pratap S., Kasi Viswanath K., Sampath Kumar R., And Dinakara Rao A.

ABSTRACT

Aedes aegypti is a vector that transmits diseases like dengue fever, chikungunya, and yellow fever. It is distributed in all tropical and subtropical regions of the world. According to WHO reports, 40% of the world's population is currently at risk for dengue fever. As vaccines are not available for such diseases, controlling mosquito population becomes necessary. Hence, this study aims at UDP-N-acetyl glucosamine pyrophosphorylase of *Aedes aegypti* (AaUAP), an essential enzyme for chitin metabolism in insects, as a drug target. Structure of AaUAP was predicted and validated using *in-silico* approach. Further, docking studies were performed using a set of 10 inhibitors out of which NAG9 was found to have good docking score, which was further supported by simulation studies. Hence, we propose that NAG9 can be considered as a potential hit in designing new inhibitors to control *Aedes aegypti*.

Keywords: *Aedes aegypti*, Chitin Metabolism, UDP-N-Acetyl Glucosamine Pyrophosphorylase, Amino Sugar, Docking and Simulation Studies.

1. Introduction

Insects are most diverse and abundant of all terrestrial animals. Insects dominated the earth by successfully adapting to wide range of ecosystems. As part of the ecosystem, they compete for food with other biota and in turn cause various infections to vegetation, livestock, and humans. Though chemical pest control is a predominant type of method to control pests, it causes threat to other biota. Hence, there is a constant need to identify specific insect drug targets. Chitin metabolic pathway is essential for the growth and development of insects and inhibition of enzymes involved in the pathway will help in controlling insect growth. Chitin metabolising enzymes are present only in invertebrates like insects and absent in vertebrates [1]. Because of the absence of chitin metabolic pathway in higher plants and mammals, and its biological necessity in insects, chitin metabolism represents a rather selective target for insect control agents [2-4]. Chitin (C₈H₁₃O₅N)_n is the most widespread amino polysaccharide and important biopolymer in nature. It is a linear homopolymer of the sugar, N-acetyl glucosamine (a derivative of glucose), connected by β-1, 4-linkages. It is the second most abundant organic compound in nature after cellulose and an important structural component of the cell wall of many fungi and certain algae, the exoskeleton and peritrophic matrix of insects and crustaceans, and the shell of mollusks and nematode eggs [1]. Insect cuticle is rigid due to the presence of chitin and sclerotized proteins. To allow growth and development, insects periodically replace their old cuticle with a new one during molting (ecdysis). Insect molting requires strict control of the chitin metabolizing enzymes during development. Because of the importance of chitin in growth of insects, chitin synthesizing enzymes were assumed to be excellent targets for pest control agents and chemical insecticides. Although chitin metabolism has biological significance, relatively little information is known about the chitin metabolic pathway in insects or other invertebrates. The chitin metabolic pathway begins with the production of glucose from the cleavage of trehalose by trehalase, followed by series of chemical reactions catalyzed by various enzymes leading to the formation of chitin. The last step in the chitin biosynthetic pathway is catalyzed by chitin synthase (CHS), a key enzyme in chitin metabolism, which catalyzes the polymerization of chitin from activated UDP-N-

acetylglucosamine monomers. The two primary enzymes responsible for chitin degradation in insects are chitinases and β -N-acetylglucosaminidases. [1]

CHSs and chitinases have been extensively studied in fungi and in several other insects [5, 6]; in contrast to these, other enzymes of chitin metabolism were characterized in very few insects [7, 8]. Enzyme, UDP-N-acetylglucosamine-pyrophosphorylase (UAP), belongs to the family of transferases. UAP catalyzes the step immediately preceding CHS in the chitin biosynthetic pathway. The UAP's supply activated precursors of sugars needed for the biosynthesis of sugar polymers, glycoproteins or other glycoside conjugates [9]. This enzyme is essential for insect survival, and is required for cuticle organization, tracheal tube morphogenesis and glycosylation of proteins. Inhibiting the enzymes activity will stop insect growth [10]. The UDP-N-acetylglucosamine (UDPGalNAc) is a key precursor in chitin biosynthesis of insects. This precursor is formed as a result of the reaction between N-acetylglucosamine-1-phosphate (NAGP) and uridine-5-triphosphate (UTP), catalyzed by the enzyme UDP-N-acetylglucosamine pyrophosphorylase (UAP) [11]. The inhibition of UDP-N-acetylglucosamine formation affects the synthesis of chitin. Therefore, insect exoskeleton synthesis cannot take place, which results in insect death.

So, structural characterization of these enzymes will be helpful in better understanding of chitin metabolism and identifying suitable compounds, which can inhibit these enzymes. As crystal structure is absent for insect UAP, *in-silico* methods were used for the structural characterization of this enzyme in *Aedes aegypti*.

Aedes aegypti is a vector that transmits diseases like dengue fever, chikungunya, and yellow fever. It is distributed in all tropical and subtropical regions of the world. Currently 40% of the world's population is at risk for dengue fever (WHO 2009) (<http://www.who.int/mediacentre/factsheets/fs117/en/>).

Human activities also lead to rapid growth of mosquito populations. As vaccines are not available for diseases like dengue fever, controlling mosquito population is a necessity [12]. Hence, the present study includes structural characterization and docking studies on *Aedes aegypti* UAP (AaUAP).

2. Material and methods

2.1. Homology modeling

AaUAP protein sequence (Accession Number: XP_001659746) was retrieved from NCBI (<http://www.ncbi.nlm.nih.gov/>). The template (PDB ID: 1JV1) used to build the 3D model was retrieved from Protein Data Bank (<http://www.rcsb.org/>). MODELLER9v10 [13] was utilized to align and model the AaUAP protein. The sequence alignment between the template 1JV1 and AaUAP was performed using ClustalW [14] for identifying the conserved regions. A total of 20 models were generated and the best model was selected based on the discrete optimized protein

energy (DOPE) scoring function [15, 16]. The validation of the models was carried-out using SAVES server (<http://nihserver.mbi.ucla.edu/SAVS/>), which evaluates the 3D structure quality of the protein using PROCHECK [17], ERRAT [18], and Verify3D [19]. For structural insights, Chimera [20], visualization tool, was used.

2.2. Ligands for Docking

The ligands used for docking studies include UTP, NAGP, UDPGalNAc and a set of ten inhibitors namely NAG1-NAG10 obtained from earlier study [21]. The 2-dimensional structures of UTP, NAGP, and UDPGalNAc were represented in Figure 1 and the structures of all the inhibitors (NAG1-10) used for docking were shown in the Figure 2. The 3D structures of all the compounds were prepared using ChemSketch software (www.acdlabs.com).

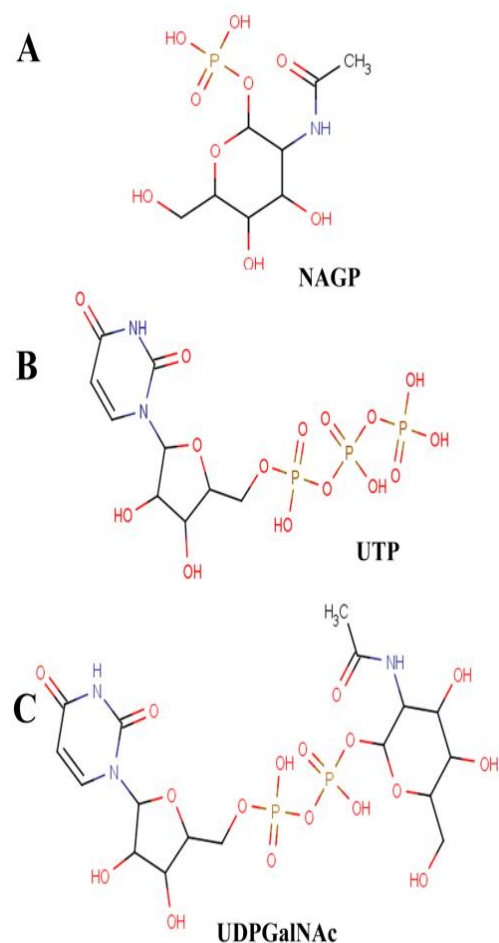


Fig 1: Schematic representations of 2D images of ligands used in this study

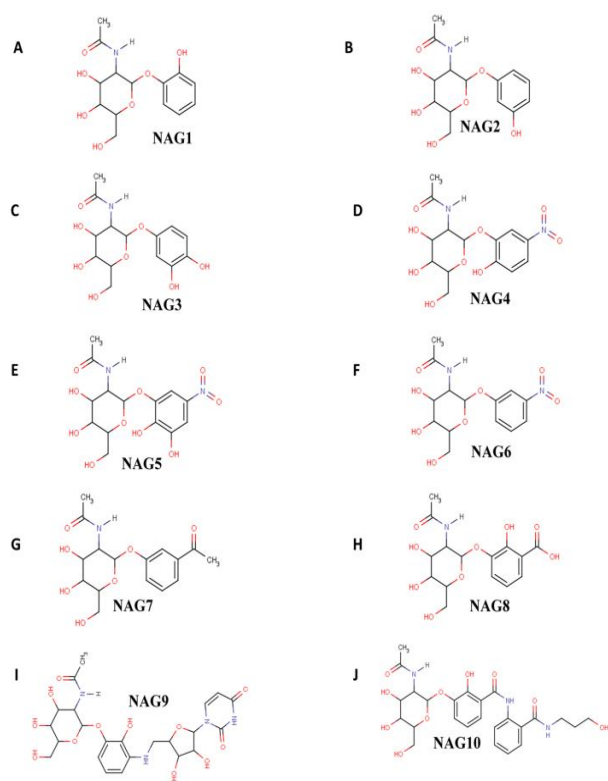


Fig 2: (A-J) Schematic representations of 2D images of inhibitors used for docking

2.3. Molecular docking studies

2.3.1. Preparation of protein

Molecular docking studies were performed using Schrodinger Maestro (version 9.2; Schrödinger LLC, New York). To gain insights into the binding cavity of AaUAP, docking was performed between AaUAP–UTP (substrate), AaUAP–NAGP (substrate), AaUAP–UDPGalNac (product), and AaUAP–inhibitors. Initially, AaUAP model was preprocessed using protein preparation wizard of Schrodinger and subsequently energy minimized using OPLS force field.

2.3.2. Preparation of Ligands

All the ligands were prepared using Lig Prep (version 2.3, Schrödinger Inc.) module with default parameters. Bond orders were assigned and various ionization states, tautomers, stereochemistries, and ring conformations were produced for each input structure. The structures were minimized using OPLS-AA force field. These structures were used for Glide (grid-based ligand docking with energetics) docking.

2.3.3. Receptor grid generation

A receptor grid was created around the protein active site by selecting the key residues reported in the literature^[21-23]. Grid box size was set at 20 Å × 20 Å × 20 Å and Vander Waal radii of receptor atoms were scaled to 1.00 Å with a partial atomic charge of 0.25.

2.3.4. Protein - Ligand Docking

All docking calculations were performed using the “Standard Precision” (SP) mode of Glide docking (version 4.5,

Schrödinger Inc.). A scale factor of 0.8 and partial atomic charge of less than 0.15 was applied to the atoms of protein for van der Waals radii. The number of poses generated for each ligand was set to 10,000 and out of them 10 best poses per ligand were chosen for energy minimization. The best docked structure from each docking calculation was chosen based on Glide Score function. The interactions of the docked complexes were further studied.

2.4. Molecular Dynamics Simulations (MDS)

MDS were carried out using GROMACS distribution 4.5.6^[24]. Protein topologies were created using GROMACS and ligand topologies were built using PRODRG Server^[25] (<http://davapc1.bioch.dundee.ac.uk/cgi-bin/prodrgr>). The system was embedded in a cubic box of simple point charge (SPC) water model and neutralized by replacing solvent molecules with Na⁺ and Cl⁻ ions. The final system containing approximately 39,542 residues was set with periodic boundary conditions, the Particle Mesh Ewald (PME) method^[26]. Energy minimization was performed using steepest descent for 1000 steps. MDS consist of equilibration and production phases. The equilibration phase is conducted under two ensembles NVT (constant Number of particles, Volume, and Temperature) and NPT (constant Number of particles, Pressure, and Temperature). Initially, the solvent atoms and ions were equilibrated using NVT ensemble at 300K temperature for 100 ps until all the atoms attained the set temperature and proper orientation was established between solute and solvent molecules. Temperature coupling was done using V-rescale; modified Berendsen thermostat^[27]. Later, the system is equilibrated with NPT ensemble at 1bar pressure for 100 ps. Pressure coupling was done using Parrinello-Rahman barostat^[28]. Final MDS was run at 300K temperature and 1 bar pressure. Periodic boundary conditions were applied and motion equations were unified using leaf-frog algorithm. Results of the simulations were analyzed using xmgrace tool.

3. Results and Discussion

3.1. Homology Modeling

Template search for homology modeling of AaUAP yielded 1JVI as the suitable structural template with 99% query coverage and 52% sequence similarity. Based on the structure of 1JVI, 20 models were built and out of them, the model having least molPDF score of 3525.65381 was considered for further validation. Validation results revealed that 91.6% of residues were in most favored regions (Figure 3A). The overall quality of the predicted structure was found to be good, which is evident from the higher ERRAT value of 78.225. VERIFY_3D analysis reported 97.11% of amino acid residues had an average 3D-1D score > 0.2, indicating optimum primary sequence to tertiary structure compatibility (Figure 3B). The RMSD value of the model was found to be less (0.775Å) when superimposed with the template backbone, suggesting the high quality of the model. Sequence alignments carried out showed that most of the residues were conserved (Figure 4). Since all the validation results found to be good, the modeled insect AaUAP was considered reliable. The AaUAP structure consists of 23 helices and 22 strands

(forming 7 sheets) comprising three domains i.e., an N-terminal domain, a large central domain and a C-terminal domain. Central domain forms a Rossmann Fold, which contains an eight stranded β -sheet surrounded by eight α -helices and a small two stranded β -sheet at one end (Figure 5).

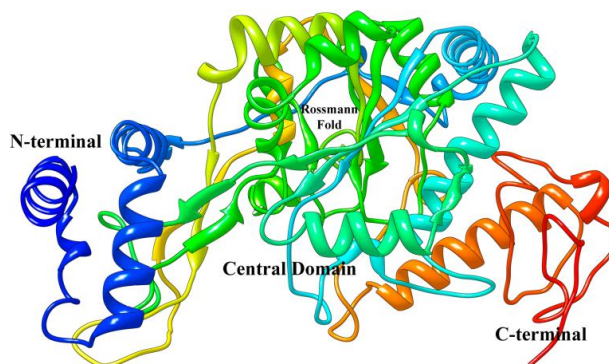


Fig 5: The representation of 3D model of *Aedes aegypti* UDP N-acetyl glucosamine pyrophosphorylase (AaUP).

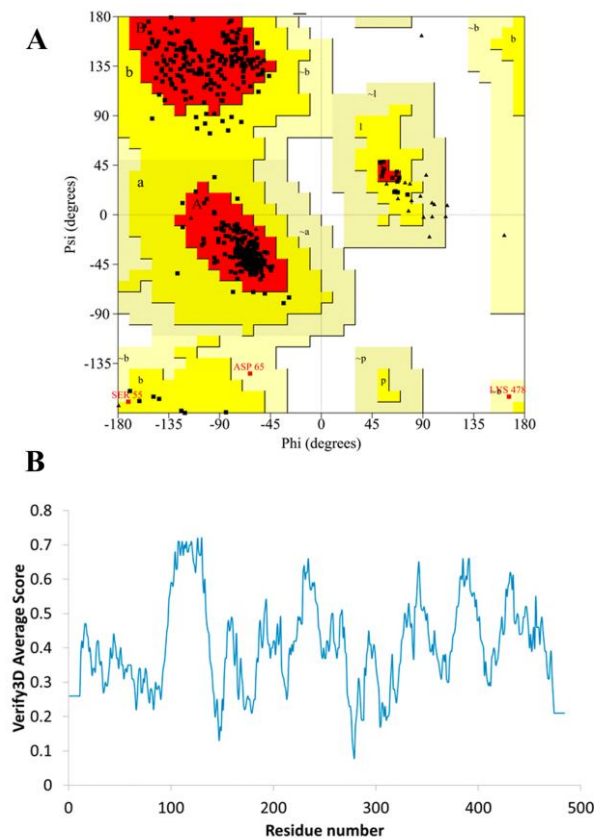


Fig 3: Validation results for the modeled protein A) The Ramachandran plot and B) The Verify3D plot

1JV1	--NINIDLKLTLSKAGQEHLRLFWNELERAAQVLEYAELQAMNFEELNFFTCQAIKRGFNS	59
AaUP	MNLDLAKTSLAKHQDQLQYWEELDRDRRLTEDIDELNLEEVNFFKRAATSLLEG	60
1JV1	SHQKVDARMEVFRVFLGSATRD--QDQLQANESEGLFQISQNKVAVLLLAGGGQTRLGV	118
AaUP	--NAKLDDKMEVFCEDKFLSISRTTDDQLKHYEGLRQIADGKVGVLIMAGGGQTRLGF	118
1JV1	AYPKGMVDGLPSKRTLFQIQARILKIQVAEKYVGNKCIIPWYINTSGRMTSEKFF	178
AaUP	AFPKGMFVGLPSKSLFRIQGERILKLRLAELTGTGRITWYINTSBHTMPTKKYF	178
1JV1	TKHKYFGLKKNVIFQGGMLPAMFDGKIILEKNKVSMAFDGNGGLYRALAAQIVED	238
AaUP	EENDYFGLKAEIDIMPEQGSDFCYDFEGKILLDEKRVAKAPDNGGLYRALDRGILDD	238
1JV1	MEQRGWSIHVYVDNLLVKVADPRFIFGCIQKGDGCAKVEKTNPTPEVGVVCRVDGV	298
AaUP	LERRGVLYLHAHSDNLLIKVADPVSIGYFVEQKADCAKVEKSHFNEAVGVVQVDGK	298
1JV1	YQVVEYSEISLATAQRSSDGRLLFNAGNIANHFFTVFPLRDVNVVYEPQLQHHVAQKI	358
AaUP	YQVVEYSEITQRTAELRKEDGRLVFNAGNICNHFFTSFLRKIGTTFEKDLKLVHAKKI	358
1JV1	FVYDTQGLIKPDKFNKIMEKVFVDIFQFAKKFVVYEVLRDEFSFLKNADSQNGKDP	418
AaUP	FFIDSTGTRCTPDKFNKIKIEKVFVDFQFAEHFVTIEVFRDEEFSALKNADS--AKRCA	417
1JV1	TTARHALMSLHCWVINAAGGHFIDENGRSLFAIPLKIDANDVFIQCEISPLISVAGEGLE	478
AaUP	TTARADITRLHKRYTEAAGG--TVGGT-----ECRISPLISVSGEGLK	458
1JV1	SYVADKEFHAF--LIIDENGVHELKNGI	505
AaUP	VLVKGRTEVSPVHMADEEKSEVVE--	484

Fig 4: Representation of sequence alignment of the template (1JV1) and target (AaUP)

3.2. Molecular Docking Studies

UAP was chosen as a therapeutic target for controlling insect growth. As there is lack of information about the binding site of insect UAP, the active site residues were defined in accordance to the earlier studies on UAP [21, 22]. The active site residue numbers of AaUP were identified by aligning the AaUP protein sequence with the template sequence. The sequence alignment displayed that the conserved active site amino acid residues of AaUP aligned with the active site residues of 1JV1. Docking studies were performed by assigning G111, G112, Q196, G222, N223, D253, G290, E303, Y304, N327, F381, F383 and Lys407 as active site residues. AaUP was docked with UTP, NAGP, UDPGalNac, and 10 inhibitors. The binding modes of the docked compounds were ranked according to Glide score. The most favorable binding modes of all the docked compounds were selected for further analysis. The Glide score, Emodel score and the key interacting residues of the docked complexes were listed in Table 1.

The docking results revealed that the binding pocket of AaUP was found to be considerably hydrophobic. To understand the mechanism of substrate binding, the AaUP was initially docked with UTP, the first substrate that enters the active site [29], and then the docked AaUP-UTP complex was used for docking with NAGP. The docking results showed that, the UTP is making contact with the two conserved regions Gly110 to Gly118 and Asp221 to Leu226 and forming hydrogen bond interactions with G110, G113, T114, L116, K122, and Q196 which was in accordance to the earlier study. NAGP established hydrogen bond interactions with Y304, K407, and N223 and hydrophobic interactions with F381 and F383, which were also found to be conserved in template structure. Residues forming other interactions were listed in Table 1. Docking of UDPGalNac with AaUP revealed that the UDP moiety is forming hydrogen bond interactions with G113 and other interactions with residues of conserved nucleotide binding loop G110, G111, Q112, T114 R115, L116, P121, and K122. The amino sugar moiety formed hydrogen bond interactions with residues N223, N327, G290, and K407.

Table 1: Docking results and interacting residues of the ligands NAGP, UTP, UDPGalNac, and NAG9

S. No	Name of The Protein – Ligand Complex	Glide Score (Kcal/Mol)	Glide Emodel Score	Interacting Residues
1	UAP-UTP COMPLEX	-8.811	-69.261	M108, A109, G110, G111, Q112, G113, T114, R115, G117, L116, F118, K122, M165, Q196, P220, G222, N223, S251, V252, D253, and K407
2	UAP-UTP-NAGP COMPLEX	-8.782	-102.582	M108, A109, G110, G111, Q112, G113, T114, R115, L116, G117, F118, K122, M165, Q196, P220, G222, N223, S251, V252, D253, A288, V289, G290, E303, Y304, N327, I328, C329, F381, V382, F383, F403, and K407
3	UAP-UDPNACEGLN COMPLEX	-8.170	-125.945	G111, Q112, G113, T114, R115, L116, F120, P121, K122, N223, S251, D253, A288, V289, G290, V301, E303, Y304, N327, I328, C329, F381, F383, F403, A405, and K407
4	UAP-NAG9 COMPLEX	-7.43	-95.40	G111, Q112, G113, T114, R115, L116, G117, F118, A119, F120, P121, K122, H169, T170, A219, P220, D221, G222, N223, E303, Y304, K356, K377, E379, F381, and K407

Out of the ten inhibitors docked, NAG9 showed better binding efficiency than others, which is evident from lower Glide score (-7.43 Kcal/mol) and hence NAG9 was analysed further. The NAG9 was found to have hydrogen bond interactions with residues T114, L116, K377, and E379. From the analysis it was observed that all the compounds (UTP, NAGP, UDPGalNac, and NAG9) were interacting with identical sets of amino acids suggesting the good binding affinity of the

designed inhibitor NAG9 towards the AaUAP. It was observed that except the active site residues G117, F118, A119, H169, T170, and A219 all other residues were found to be interacting with UDPGalNac. This large number of overlaps in interacting residues may be due to the fact that UDPGalNac shares structural similarity with NAG9 compared to other inhibitors. The representations of binding modes of the compounds UTP, NAGP, UDPGalNac, and NAG9 were given in Figure 6.

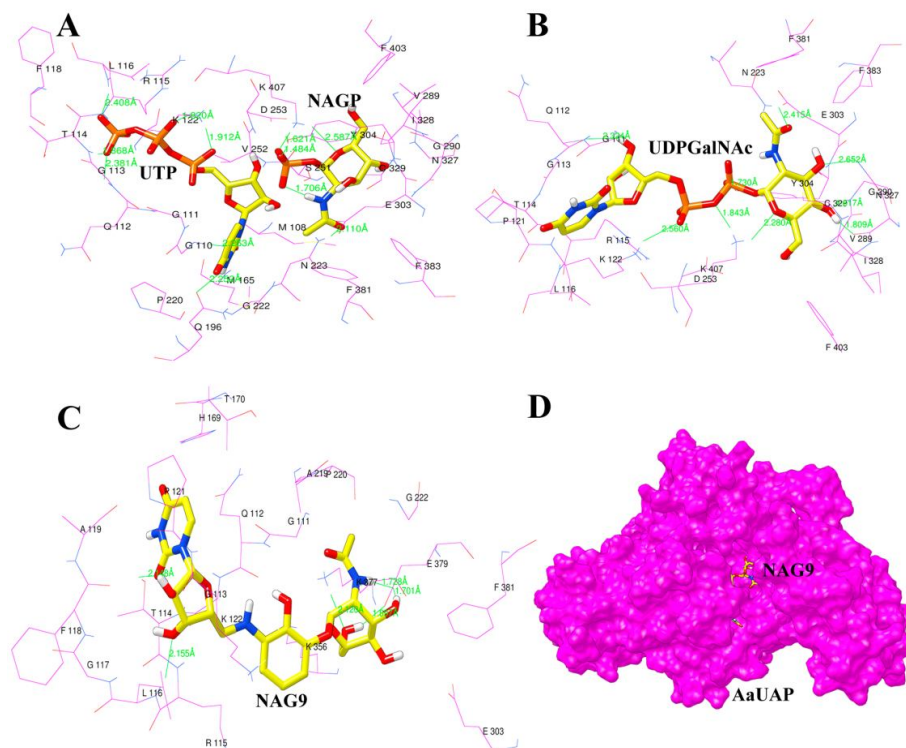


Fig 6: Binding modes of the complexes of AaUAP with A) NAGP and UTP, B) UDPGalNac, C) NAG9 and D) The surface representation of the protein AaUAP with NAG9 in the active site

The ligand interaction plots generated from all the docked complexes revealed that residues G111, Q112, G113, T114,

R115, L116, F120, K122, N223, F118, G222, E303, Y304, F381, and K407 were showing interactions with almost all the

compounds used for docking and sequence alignments with template and other insect UAPs (data not shown) revealed that all these residues were highly conserved, which signifies that these residues are important for the catalytic activity of AaUAP and other insect UAPs.

3.3. Molecular Dynamics Simulations (MDS)

MDS were performed for the protein (AaUAP) and also for the best docked poses of both the substrate (AaUAP-UTP-NAGP) and inhibitor (UAP-NAG9) complexes to check the stability and to get insights into conformational and behavioral changes over a time period. The modeled AaUAP protein, AaUAP-UTP-NAGP and AaUAP-NAG9 complexes were subjected to MDS for a time period of 10 ns, 5 ns and 5 ns respectively. MDS revealed the structural and functional characteristics of all the models. Root mean square deviation (RMSD), root mean square fluctuations (RMSF), and radius of gyration (Rg) of the system were observed. RMSD of AaUAP protein model with respect to the starting model disclosed that the deviation was maintained below 0.3 nm throughout the 10 ns time

period (Figure 7A). Similarly, The RMSD of AaUAP-UTP-NAGP and AaUAP-NAG9 complexes showed that the oscillations increased slowly in the initial 2 ns time period, but later attained stability and maintained below 0.3 nm throughout the simulation time period (Figure 7B). Similar RMSD of inhibitor complex compared to substrate complex specifies that the inhibitor formed a stable complex with AaUAP. It was observed that the RMSF of all the residues in AaUAP, AaUAP-UTP-NAGP, and AaUAP-NAG9 complexes were less fluctuating, which strongly suggests that the structures are stable and accurate (Figure 7C and D). Initially the Rg of AaUAP was found to be increasing, but decreased after 2 ns and attained stability after 8 ns, suggesting that the compactness of the protein increased during simulation. The Rg values of AaUAP-UTP-NAGP and AaUAP-NAG9 complexes were found to be decreased during the 5 ns simulation time period (Figure 7E and F), which indicates that the substrate and inhibitor were responsible for conformational changes in AaUAP.

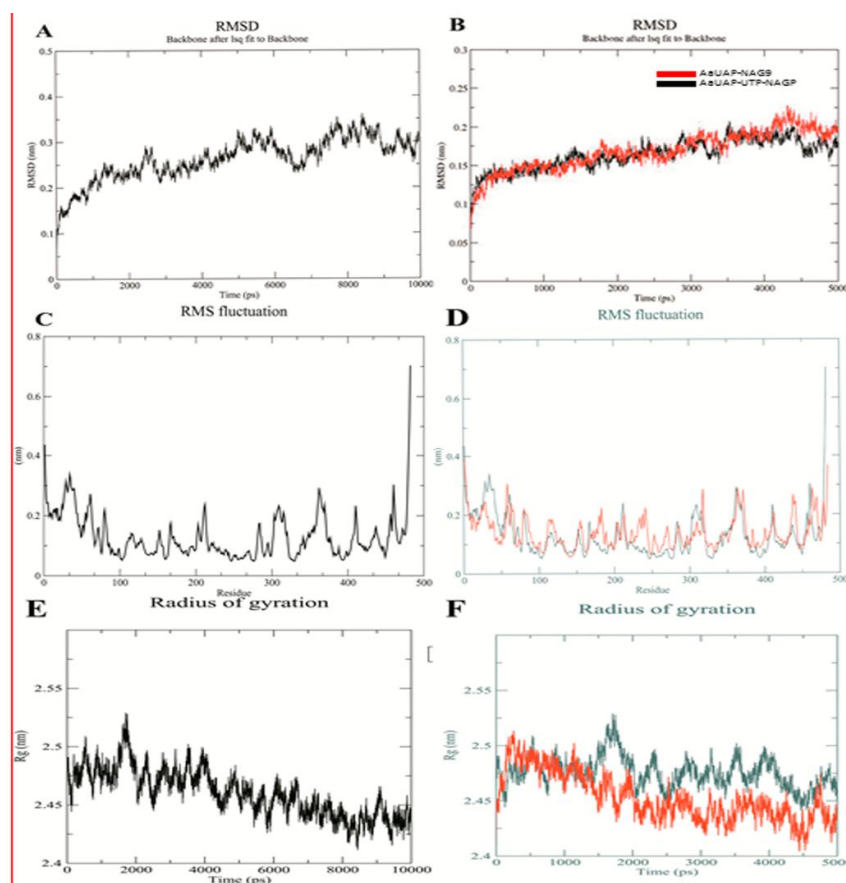


Fig 7: (A-F) Molecular dynamic simulation results of AaUAP (A, C and E), AaUAP-NAG9-UTP and AaUAP-UDPGalNac (B, D and F)

Docking studies provided information on active site of AaUAP and efficiency of NAG9 as an AaUAP inhibitor. Further, the MDS results were also found to be supporting this. Hence, NAG9 can be considered as a new hit for designing new drugs for inhibiting AaUAP.

4. Conclusion

Aedes aegypti is widely distributed in the tropical and subtropical regions of the world. Infections spread by this mosquito are of major health concern worldwide. As the mosquito is developing resistance against the currently available drugs, there is an urgent need to find new targets and

drugs to control the growth of the *A.aegypti*. Hence, a novel target, AaUAP (which is involved in chitin bio-synthesis), was chosen in this study. The 3D structure of AaUAP was modeled and the validation procedures suggest that the designed model was reliable, which was also confirmed through molecular dynamics simulations over a period of 10 ns. Molecular docking studies revealed NAG9 as the best hit in inhibiting AaUAP, which was supported by molecular dynamic simulation study. Hence, NAG9 was considered as potential hit and could be used as a preliminary structure for designing new drugs.

5. Acknowledgment

Authors thank University Grants Commission (UGC, F.No. 42-206/2013), Government of India for financial support and Centre for Bioinformatics, Pondicherry University for providing necessary computational facilities to carry out the research work.

6. References

- Merzendorfer H, Zimoch L. Chitin metabolism in insects: structure, function and regulation of chitin synthases and chitinases. *Journal of Experimental Biology* 2003; 206(24):4393-4412.
- Kramer KS, Muthukrishnan L, Johnson F. White. Chitinases for insect control. *Advances in Insect Control: The Role of Transgenic Plants*. Taylor and Francis Publ. Bristol, PA 1997, 185-193.
- Arakane YS, Muthukrishnan K, Kramer C, Specht Y, Tomoyasu M, Lorenzen *et al*. The *Tribolium* chitin synthase genes *TcCHS1* and *TcCHS2* are specialized for synthesis of epidermal cuticle and midgut peritrophic matrix. *Insect molecular biology* 2005; 14(5):453-463.
- Spindler KD, Spindler-Barth M, Londershausen M, Chitin metabolism: a target for drugs against parasites. *Parasitology research* 1990; 76(4):283-288.
- Arakane YS, Muthukrishnan, Insect chitinase and chitinase-like proteins. *Cellular and Molecular Life Sciences* 2010; 67(2):201-216.
- Merzendorfer, H. The cellular basis of chitin synthesis in fungi and insects: common principles and differences. *European Journal of cell biology* 2011; 90(9):759-769.
- Horsch MC, Mayer U, Sennhauser DM, Rast. β -N-Acetylhexosaminidase: A target for the design of antifungal agents. *Pharmacology & therapeutics* 1997; 76(1):187-218.
- Zen KC, HK, Choi, N. Krishnamachary, S. Muthukrishnan, KJ. Kramer, Cloning, expression, and hormonal regulation of an insect β -N-acetylglucosaminidase gene. *Insect biochemistry and molecular biology* 1996; 26(5):435-444.
- Arakane YMC, Baguion S, Jasrapuria S, Chaudhari, A, Doyungan KJ, Kramer *et al*. Both UDP N-acetylglucosamine pyrophosphorylases of *Tribolium castaneum* are critical for molting, survival and fecundity. *Insect biochemistry and molecular biology* 2011; 41(1):42-50.
- Araújo SJ, H. Aslam, G. Tear, J. Casanova. Mummy /cysticencodes an enzyme required for chitin and glycan synthesis, involved in trachea, embryonic cuticle and CNS development—Analysis of its role in *Drosophilatracheal* morphogenesis. *Developmental biology* 2005; 288(1):179-193.
- Maruyama DY, Nishitani T, Nonaka A, Kita TA, Fukami T, Mio *et al*. Crystal structure of uridine-diphospho-N-acetylglucosamine pyrophosphorylase from *Candida albicans* and catalytic reaction mechanism. *J Biol Chem* 2007; 282(23):17221-30.
- Brown JE, Evans BR, Zheng W, Obas V, Barrera-Martinez L, Egizi A *et al*. Human impacts have shaped historical and recent evolution in *Aedes aegypti*, the dengue and yellow fever mosquito. *Evolution* 2013; 68(2):514-525.
- Šali A, Potterton L, Yuan F, Vlijmen HV, Karplus. Evaluation of comparative protein modeling by MODELLER. *Proteins: Structure, Function, and Bioinformatics* 1995; 23(3):318-326.
- Thompson JDT, Gibson DG, Higgins. Multiple sequence alignment using Clustal W and Clustal X. *Current protocols in bioinformatics* 2002; 2.3. 1-2.3. 22.
- Eswar NB, Webb MA, Marti-Renom M, Madhusudhan D, Eramian M, Shen *et al*. Comparative protein structure modeling using Modeller. *Current protocols in bioinformatics* 2006; 5.6. 1-5.6. 30.
- Eramian D, Shen M, Devos D, Melo F, Sali A, Marti-Renom MA. A composite score for predicting errors in protein structure models. *Protein Science* 2006; 15(7):1653-1666.
- Laskowski RA, MacArthur MW, Moss DS, Thornton JM. PROCHECK: a program to check the stereochemical quality of protein structures. *Journal of applied crystallography* 1993; 26(2):283-291.
- Colovos C, Yeates TO. Verification of protein structures: patterns of nonbonded atomic interactions. *Protein Science* 1993; 2(9):1511-1519.
- Eisenberg DR, Lüthy JU, Bowie. VERIFY3D: Assessment of protein models with three-dimensional profiles. *Methods in enzymology* 1997; 277:396-404.
- Pettersen EF, Goddard TD, Huang CC, Couch GS, Greenblatt DM, Meng EC *et al*. UCSF Chimera—a visualization system for exploratory research and analysis. *Journal of computational chemistry* 2004; 25(13):1605-1612.
- Junior MCS, Assis SAD, Góes-Neto A, Duarte ÂA, Alves RJ, Junior MC *et al*. Structure-based drug design studies of UDP-N-acetylglucosamine pyrophosphorylase, a key enzyme for the control of witches' broom disease. *Chemistry Central Journal* 2013; 7(1):1-7.
- Peneff CP, Ferrari V, Charrier Y, Taburet C, Monnier V, Zamboni *et al*. Crystal structures of two human pyrophosphorylase isoforms in complexes with UDPGlc (Gal) NAc: role of the alternatively spliced insert in the enzyme oligomeric assembly and active site architecture. *The EMBO Journal* 2001; 20(22):6191-6202.

23. Santos JMC, Gonçalves PA, Taranto AG, Koblitz MG, Góes-Neto A, Pirovani CP *et al.* Purification, characterization and structural determination of UDP-N-acetylglucosamine pyrophosphorylase produced by *Moniliophthora perniciosa*. *Journal of the Brazilian Chemical Society* 2011; 22(6):1015-1023.
24. Van DS, Lindahl DE, Hess B, Groenhof G, Mark AE, Berendsen HJ. GROMACS: fast, flexible, and free. *J Comput Chem* 2005; 26(16):1701-18.
25. Schuttelkopf AW, DM. van Aalten. PRODRG: a tool for high-throughput crystallography of protein-ligand complexes. *Acta Crystallogr D Biol Crystallogr* 2004; 60(Pt 8):1355-63.
26. Essmann UL, Perera ML, Berkowitz T, Darden H, Lee, Pedersen LG. A smooth particle mesh Ewald method. *The Journal of chemical physics* 1995; 103(19):8577-8593.
27. Berendsen HJ, Postma JPM, Gunsteren WF, DiNola A, Haak J. Molecular dynamics with coupling to an external bath. *The Journal of chemical physics* 1984; 81(8):3684-3690.
28. Parrinello MA, Rahman. Polymorphic transitions in single crystals: A new molecular dynamics method. *Journal of Applied physics* 1981; 52(12):7182-7190.
29. Mochalkin IS, Lightle Y, Zhu JF, Ohren C, Spessard NY, Chirgadze *et al.* Characterization of substrate binding and catalysis in the potential antibacterial target N-acetylglucosamine-1-phosphate uridyltransferase (GlmU). *Protein Science* 2007; 16(12):2657-2666.